DEVELOPMENT OF A SPATIAL-DYNAMICAL MODEL OF THE STRUCTURE OF TOXIC CYANOBACTERIA CLUSTERS FOR BIOSECURITY PURPOSES

Розроблено просторово-динамічну модель, що описує структуру скупчень токсичних ціанобактерій на великих водних площах. Продемонстровано застосування побудованої моделі до виявлення структури скупчення на цифрових знімках. Характер біопродукційних процесів, що визначають небезпеку скупчення токсичних мікроорганізмів, визначається рядом параметрів, які можуть бути виміряні дистанційно аерокосмічними методами (фотографуванням). Запропонована модель на підставі цифрового знімка дозволяє відновити просторово-динамічну картину скупчень шляхом визначення стану біопродукційних процесів різних частин скупчення. Інформація про такі стани має велике значення для оптимізації заходів по елімінації загроз токсичності.

Розробка даної просторово-динамічна моделі пов'язана з необхідністю виявлення структури скупчень токсичних ціанобактерій на водних площах для цілей усунення загроз біобезпеки. Такі скупчення є надзвичайно складними об'єктами і не відтворюються ні теоретичними, ні натурними моделями.

Побудована просторово-динамічна модель дозволяє виявити динамічну картину біопродукційних процесів в різних частинах скупчення мікроорганізмів. Прикладна важливість отриманих результатів пов'язана з підвищенням ефективності заходів по елімінації загроз токсичності, тобто завдяки побудованої моделі можна виявляти найбільш ефективні, з точки зору усунення загрози, ділянки.

Результат застосування моделі до цифрових знімків токсичних ціанобактерій відповідають гідробіологичним уявлення про об'єкти даного роду

Ключові слова: просторово-динамічна модель, ціанобактерії, біопродукційні процеси, колорометричні параметри, біобезпека

O. Vysotska
Doctor of Technical Sciences, Professor*
E-mail: olena.vysotska@nure.ua
M. Georgiyants
MD, Professor
Department of Pediatrics Anesthesiology and Intensive Therapy**
K. Nosov
PhD
Department of Theoretical and Applied Informatics
School of mathematics and computer science
V. N. Karazin Kharkiv National University
Svobody sq., 4, Kharkiv, Ukraine, 61022
Y. Balym
Doctor of Veterinary Science, Professor
Department of Reproductology
Kharkov State Zooveterinary Academy
Academichna str., 1, Malaya Danylivka, Dergachi district, Kharkiv region, Ukraine, 62341
A. Pecherska
PhD*
A. Porvan
PhD, Associate Professor*
S. Pavlov
PhD, Professor
Central research laboratory**
V. Shekhovtsova
PhD, Associate Professor*
T. Klochko
Senior Lecturer
Department of Chemistry, Ecology and Expertise Technology
National Aerospace University "Kharkiv Aviation Institute"
Chkalov str., 17, Kharkiv, Ukraine, 61070
A. Solodovnikov
PhD
Department of Medical and Biological Physics and Medical Informatics
Kharkiv National Medical University
Nauky ave., 4, Kharkiv, Ukraine, 61022
*Department of Information Control System
Kharkiv National University of Radio Electronics
Nauky ave., 14, Kharkiv, Ukraine, 61166
**Kharkiv Medical Academy of Postgraduate Education
Amosova str., 58, Kharkiv, Ukraine, 61176

1. Introduction

At present, global climate change and the increased impact of mankind on nature pose numerous threats to bi-osecurity. The character of these threats requires a revision of certain concepts related to the strategy for environmental activities. It is required to not only care about preserving the evolutionary-created biodiversity. There is a need to develop

tools for the use of various aspects of biodiversity in order to eliminate the specified threats. Among these tools, an important role belongs to methods of mathematical modeling. Given the task to devise these methods, one should note the new approach to the understanding of biodiversity, stated in [1] within the concept of optimal diversity. The key source of the specified, and similar, approaches can be considered the position described earlier in [2], in accordance with which an environmentalist treats each measure of diversity as an opportunity to construct a system with a feedback. A large number of different mathematical models have been built up to now for a formalized description of the structure and functioning mechanisms of these feedbacks. One can highlight among the most known models the structural equations, a path analysis, (fuzzy) cognitive maps, matrix models of population biology, continuous and discrete dynamic models of competition, and many others.

However, a series of important applications in ecology, theoretical biology, medicine, and other disciplines, require analysis of not only the internal structure of relations, but also the relations in space. Space can be both one-dimensional and have multiple dimensionalities. In response to these requirements, a separate field or research has been formed – spatial statistics, or spatial analysis, which is not identical to multivariate statistics and is based on its proprietary methods.

Application of spatial models in biosecurity is aimed at prediction and description of natural objects that represent a biological threat. The major concerns include threats to different types of water consumption. They are formed, in particular, by the eutrophication of water bodies with massive growth of toxic cyanobacteria in them. In many cases, the elimination of these threats falls into the field of veterinary medicine. We are talking about biosafety conditions for watering the livestock, grazing on coastal sites at eutrophied water reservoirs, water supply to livestock complexes. A vivid example of such a potential threat associated with the development of the agricultural economy, in a freshwater reservoir, is the situation at the Middle East Lake Kinneret. This water reservoir is the main source of drinking water for Israel; its eutrophication poses a serious risk related to the emergence of accumulations of toxic cyanobacteria in its waters. The assessment of this risk has involved a multi-year research into stability factors of the Kinneret hydrobiocenosis [3].

Similar problems have occurred at many other freshwater and marine waters. An example of this kind is the Baltic Sea, where there are clusters of toxic cyanobacteria (CTC) the size of tens of kilometers. Addressing these issues requires the application of satellite-based methods to monitor localization and displacement of CTC over a water site. To this end, there are very powerful international institutions, such as the HELCOM Commission (Baltic Marine Environment Protection Commission – Helsinki Commission) [4].

An important application of the specified satellite methods is information support of decision-making on measures for elimination of CTC. The importance of the specified application could increase significantly in case of the occurrence of particularly toxic mutants of cyanobacteria within CTC. Such mutants can form naturally. In addition, current situation in the world [5] does not make it possible to rule out a variant when the advent of such mutants might result from structures engaged in bioterrorist activity. In such situations, drastic measures to eliminate CTC would be justified. An example of such radical measures is the treatment of CTC with algaecides using aviation. That would require operative methods to search for the target – in order to detect clusters in the water area.

Modern remote (aerospace) methods enable the detection of CTC over a water area and make it possible to define, with a satisfactory level of detail, their boundaries at most. Under emergency related to the occurrence of CTC with highly toxic mutants, such information will not suffice. This is predetermined by that the efficiency of procedures to address threats of toxicity often depends on the correct determination of the structure of clusters. Thus, the efficiency of air-borne treatment of CTC with algaecides could be improved by a proper choice of sites for such an influence. It is obvious that treatment with algaecides, which suppress the processes of cyanobacteria photosynthesis, will be most effective at areas with a high intensity of these processes. At sites with a lower intensity of bioproduction process, efficiency could be significantly smaller. For example, at areas where a bioproduction strategy of accumulation and conservation of biogenic elements due the die-out of the cyanobacteria biomass is implemented. On the other hand, sites with a different character of bioproduction processes can vary in conditions and likelihood for the introduction of highly toxic mutants to CTC.

Therefore, the development of methods for detecting within CTC the sites with a different character of bioproduction processes is important from the standpoint of biosecurity. In this case, bioproduction processes at these sites are an important aspect of biodiversity and are also of interest from the viewpoint of basic biology. An important aspect of such methods is their remote character, which makes it possible to carry out research using aerial and space photography. It is a relevant task to develop of such methods in order to study the clusters of toxic cyanobacteria.

2. Literature review and problem statement

The basic method for studying bioproduction processes over large areas is the remote sensing. Primarily, this relates to that laboratory and field research methods incur considerable temporal, financial, organizational, and other costs, sometimes rendering research impossible. In this regard, significant results were obtained for terrestrial plant communities. Paper [6] generalized results of the application of remote sensing methods for determining the character of bioproduction processes at land plots in the south of Western Siberia where agricultural crops are cultivated. Study [7] demonstrated a possibility for isolating the plots of crops of perennial grasses with different parameters of bioefficiency by using remote optical methods. The results of application of remote sensing methods for finding the degraded forest areas with a reduced biological productivity were reported in [8]. However, these methods are not suitable for the bioproduction processes in water arrays due to specificity of the latter.

A significant success has been achieved when using remote methods to examine the bioproduction processes within phytoplankton communities at marine and continental water reservoirs. Paper [9] report results that demonstrate a possibility to highlight, based on the remotely determined colorimetric attributes, the areas in an ocean with a different character of bioproduction processes related to the functions and forms of carbon compounds.

Work [10] proposed a new mathematical model for detection of accumulations of toxic cyanobacteria – a descriptive binary model (DBM). Even though a given model is designed for describing dynamic systems whose components are measured at the simplest scale, dichotomous, it has several important advantages. The model makes it possible, based on the observations, which lost a temporal arrangement, to restore that order, and to describe the relationships among components that generate the dynamics of the system. Applied to the task on detecting CTC, a given model, as shown in [10], identifies a cluster based on a digital image taken under conditions of poor visibility. However, the structure of the cluster, which reflects the dynamics of bioproduction processes, cannot be identified. This is due to the very character of the model, its dynamics and a dichotomous scale of measurement, which make it impossible to identify the required properties of a cluster. Paper [11] proposes, in order to improve conditions for remote detection of CTC at a water area, to process its image using discrete models of dynamic systems (DMDS). The application of DBM and DMDS creates additional possibilities for reducing requirements to the methods of direct measurement of primary colorimetric parameters. We are talking about the colorimetric parameters of CTC, as well as the plots of surrounding water free of them. Study [11] employed primary colorimetric parameters related to the content of chlorophyll, as well as red and yellow-orange plant pigments. Given this, values for these parameters are related to the character of bioproduction processes in the examined system. Building on the approach described in [11], it is possible to suggest interpretation of different combinations of these values, which are represented by phases in the identified dynamic process as the manifestation of certain strategies for bioproduction processes. The actual material required for the identification of a dynamic process can be acquired from a computer-based analysis into parameters of the RGB-model of a digital photography. In this case, images of sites at water area with CTC can be derived using relatively simple and cheap modifications of drones, by employing their embedded equipment for digital photography. Thus, the specified results could identify the dynamics of bioproduction processes of CTC, but not the spatial structure of clusters.

It is known that research into bioproduction processes in the clusters of cyanobacteria is very difficult. As noted in [4], CTC are complex natural objects. They cannot be properly reproduced via experimental or theoretical models due to the complexity of relationships among many non-permanent relevant factors. Paper [12] noted that given the considerable mobility and dynamic of clusters, remote sensing methods make it possible to satisfactorily define only the border area of CTC. Recognition of the structure of cyanobacteria clusters, which matches the character of bioproduction processes, is not yet possible when using existing remote methods. A variant to overcome associated difficulties could be a construction of the spatial model of a cyanobacteria cluster, which takes such a structure into consideration.

Spatial models are widely used at present in a variety of areas in which it is important to study the spatial distribution of properties, attributes, parameters, and characteristics [13].

Such models are most widely used in geo-informational systems [14], where a modeled object implies a spatial object. A spatial object is typically defined as a representation (model) of an actual object, containing its position and a set of attributes. In geo-informational systems, spatial objects are the abstract representations of actual objects and are the subject of informational simulation. However, the geo-informational systems mostly address tasks on spatial analysis (manipulation of spatial and attributive data upon requests, implementation of operations in computational geometry, analysis of overlays, construction of buffer zones, network analysis, analysis of spatial distribution of objects), without taking into consideration dynamic changes in the analyzed objects.

In addition to geoinformatics, spatial models are commonly applied in various sectors of economy, ecology, geography, and astronomy. We shall mention only certain fields associated with models of this type.

Paper [15] studied the spatial interpretation of the known Bertrand model – a model of price competition in oligopolistic market. This model investigated the product differentiation competition under conditions when all firms compete with all. The size of cities and concentration of consumers do not have to be identical, and the model produces the unified and easily defined Nash equilibrium. A given model is dynamic; it, however, similar to many models of competition, is used to find stable, equilibrium states, which represent fixed points in a state space. Meanwhile, for natural systems, other types of dynamic are often important. For example, in the classic Lotka–Volterra model (a predator-prey model), one of the important types of behavior is the oscillatory, close to periodic, dynamics of components, in which the character of interaction between a predator and a prey manifests itself.

Spatial models are employed in environmental studies when examining the distribution of species and populations. Paper [16] constructed a spatial-temporal model for a pyrophytic bush (*Ulex parviflorus*) at the Mediterranean coast, which establishes a dependence of growth curve for individuals bush species and their spatial arrangement. The spatial pattern in the arrangement of bushes is not accidental; it is managed by a certain biological mechanism. That paper employed an apparatus of spatial point stochastic processes, which is extension of the theory of stochastic processes to the structures of spaces of a rather general type the locally compact Hausdorff spaces, whose details are given in [16]. A given stochastic apparatus is used for the simulation of growth of agricultural crops, forests, and similar objects, when it is required to explore the changing characteristics of fixed or inactive objects, for example, the structure of tree stand in the course of forest growth. However, the specified stochastic processes are of little value to CTC, which are very mobile objects, located at the water surface.

Paper [17] built a spatial model of the regulatory function for ecosystem in the marshes of Huanghai Lake (China). The mathematical model is a complex dynamic system that is described by functional, difference, and regular differential equations. Application of the model makes it possible to numerically explore the dynamics spatial and temporal changes in the regulatory function of the marshland ecosystem in order to study the effect of agriculture and fishing on the ecosystem. However, the models from [17] do not apply to CTC due to their specificity, making it possible for them to explore only the described phenomena.

Spatial models are traditionally used in epidemiology. Paper [18] employed, in order to model the propagation of Ebola virus, a chamber gravity model, given in the form of a system of regular differential equations. The chamber

structure of each country includes a series of dynamic components, associated with the spread of the virus – the number of susceptible patients, bearers of latent forms, those who recovered, etc. A spatial component of the model is a three-focal gravity model, including a chamber model, in which spatial coordinates of the capital are used as the spatial center of population. Thus, a given example employs a hierarchical structure when studying this phenomenon. The model makes it possible to model the spread of the virus at various levels – regional, nation-wide, and to predict responses to different types of intervention through the parameters embedded in the model, as well as to take into consideration stochastic factors, etc.

As mentioned, spatial modelling includes a wide set of methods appropriate to the specific phenomena studied. Commonly used tools in econometrics, epidemiology, ecology and other fields are the generalized linear mixed model, a spatial autoregression, and others. These models, when applied to spatial phenomena, make it possible to calculate the parameters (for example, regression coefficients) based on spatial data, and to produce an optimal forecast for plots for which data are not available. However, as noted in [19], obtaining high accuracy of the forecast and checking adequacy of the model to the examined phenomenon very often require finding a dynamic process that generates the spatial distribution. For example, the same work [19], among other examples, refers to study [20], according to which morbidity in wild nature is defined by a pattern in the displacement of a parasite species over the area of habitat. By knowing such a pattern, one can predict the spread of a disease much easier and more accurately than when constructing a statistical model only. Paper [19] refers to differential equations in partial derivatives (deterministic and stochastic) as a dynamic process suitable for many occasions. However, results from [19] cannot be directly applied to the task on identifying the structure of CTC. This is due to the lack of models, based on differential equations, that could satisfactorily describe the structure of CTC. In addition, such models typically make it possible to explore the dynamics of objects that they describe only qualitatively (determining asymptotic behavior, stability, etc.), while they are not suitable for the identification of a structure.

Thus, a spatial-temporal (or spatial-dynamic) model often has higher predictive qualities than the purely statistical model. This allows us to suggests that the spatial-dynamic model of a cyanobacteria cluster, provided the adequate choice of a dynamic process that defines the properties of a given object, would make it possible to obtain a model that could accurately enough reproduce production processes within CTC.

3. The aim and objectives of the study

The aim of this study is to construct a spatial-dynamic model of the structure of a cluster of toxic cyanobacteria. Such a model would enable an analysis of the structure of a cyanobacteria cluster, and to identify the areas of accumulation where it could be most appropriate to implement measures for eliminating biothreats. Given significant dimensions of CTC, one can expect that such an optimization would considerably bring down the cost of methods for dealing with the biothreat emanating from CTC.

To achieve the set aim, the following tasks have been solved:

– to acquire colorimetric parameters for a digital photograph of CTC that would define the character of bioproduction processes in a cluster of toxic microorganisms;

– to devise a procedure for the identification of spatial objects in a two-dimensional domain within the bounds of CTC, based on a digital photograph of this domain using the DMDS model;

– to verify the model constructed by using a digital image of the cluster of microorganisms and to derive practical conclusions aimed at organizing activities for eliminating the biological threat posed by CTC.

4. Method for detecting the spatially-dynamic structure of a flowering stain using the discrete dynamic model DMDS

When constructing any spatial-dynamic model, one must choose the type of dynamics and a technique for the interplay between the dynamics and a spatial structure. The dynamics, defined based on a state space and transition functions of the dynamic system, can be deterministic, stochastic, continuous, discrete, or mixed. A spatial structure is determined by the selected spatial objects that match the actual objects.

This study, when building a spatial-temporal model of CTC, was based on the DMDS model, which is a discrete dynamical model with deterministic state transitions, determined by the internal structure of the model. We selected, as spatial objects, those segments at a digital photograph, which are matched by sites of cyanobacteria clusters located at the water surface.

In order to construct a spatial-dynamic model, we shall introduce the required concepts and designations for the DMDS model. A complete description of the dynamical model DMDS could be found, for example, in [21, 22].

Underlying the model is the assumption on that the examined system consists of N components that are denoted $A_1, A_2,..., A_N$. Each component accepts K numeric or ordered values. The ordered values cannot, of course, always be represented quantitatively. If the system's components are ordered, the values for each component are related via a linear order. We consider time to discrete, too, that is the system's state is registered at moments $t=0, 1,....$ For each component A_i, its states at moments $t=0, 1,...$ are denoted $A_i(0), A_i(1),....$ The state of the system in general, as the states of all its components, can be represented in the form of a matrix as

$$\begin{pmatrix} A_1(0) & A_1(1) & A_1(2) & ... \\ A_2(0) & A_2(1) & A_2(2) & ... \\ ... & ... & ... & ... \\ A_N(0) & A_N(1) & A_N(2) & ... \end{pmatrix}. \tag{1}$$

It is assumed that the dynamics of the system is strictly deterministic (the state at time $t+1$ is uniquely identified by the state at moment t). This implies that trajectory (1) becomes periodic starting at some point. Therefore, starting at certain point s, the submatrix (1)

$$\begin{pmatrix} A_1(s) & A_1(s+1) & ... & A_1(s+\tau-1) \\ A_2(s) & A_2(s+1) & ... & A_2(s+\tau-1) \\ ... & ... & ... & ... \\ A_N(s) & A_N(s+1) & ... & A_N(s+\tau-1) \end{pmatrix}. \tag{2}$$

produces a complete description of the system's dynamics. A positive integer $\mathcal{T}$ is a period of the trajectory.

The components of the system can be linked via the following pair-wise relations: (0, 0), (0, +), (0, −), (−, +), (0, +), (0, −). Their essence is similar to such relations, adopted in theoretical biology and ecology. For example, if components A_i and A_j are linked via relationship (−, +) (which can be written as $A_i \Leftarrow (-,\ +) \Rightarrow A_j$), this would indicate that component A_i has a positive effect on A_j, while A_j negatively affects A_i. Other relationships are determined in a similar manner.

If one designates a pairwise relationship between A_i and A_j through (ω_i, ω_j), where $\omega_k \in \{-,\ 0,\ +\}$, $(k=i, j)$, then the complete structure of relations between the system's components can be represented by a relation matrix

$$
\begin{pmatrix}
& A_1 & A_2 & ... & A_N \\
A_1 & (\omega_1, \omega_1) & & & \\
A_2 & (\omega_2, \omega_1) & (\omega_2, \omega_2) & & \\
... & ... & ... & ... & \\
A_N & (\omega_N, \omega_1) & (\omega_N, \omega_2) & & (\omega_N, \omega_N)
\end{pmatrix}. \qquad (3)
$$

Elements above the main diagonal are omitted due to the anti-symmetry of the pairwise relationships.

Papers [21, 22] introduced two types of dynamics (based on weight functions and an approach based on a minimum law by Liebig), which make it possible in the presence of initial conditions to construct a trajectory of form (1) or (2).

Identification of the system of relations based on observational data proceeds according to the following procedure.

Suppose the following table of observations was acquired from observations over the system

$$
\tilde{M} =
\begin{pmatrix}
C_{11} & C_{12} & ... & {}_{1B} \\
C_{21} & C_{22} & ... & {}_{2B} \\
... & ... & ... & ... \\
C_{N1} & C_{N2} & ... & {}_{NB}
\end{pmatrix}. \qquad (4)
$$

The observations that are in columns can be executed at any time and are not necessarily ordered for time.

We denote via P and $\tilde{P}$ the correlation matrices by Pearson (if the starting components of the system are measured along a quantitative scale) or by Spearman (that is suitable for the quantitative and ordered scale) between the rows of matrix (2) and rows of table $\tilde{M}$, respectively. We introduce a measure of proximity between matrices P and $\tilde{P}$

$$
D(P, \tilde{P}) = \sum_{i=1}^{N-1} \sum_{j=i+1}^{N} \left(\left[P \right]_{ij} - \left[\tilde{P} \right]_{ij} \right)^2.
$$

A minimization task is set

$$
D(P, \tilde{P}) \to \min,
$$

for all possible component-to-component and initial conditions for the system's state. Based on the derived component-and-component relations and initial conditions, one can build a trajectory of system (2). These initial conditions would most accurately, in the sense of measure D, describe the dynamics of the system observed in matrix $\tilde{M}$. In this case, in matrix $\tilde{M}$, as stated above, the temporal order between observations could be lost. Papers [21, 22] show the viability of such an identification procedure (in the probabilistic sense).

Thus, in order to identify the DMDS model based on initial data, we need a table of observations (4), we must select the number of levels K and other parameters, which define a specific model. Upon identification, the model can be interpreted and applied for other procedures.

Application of the model to spatial data, represented in digital images, has its own features, whose examples can be found in papers [11, 23]. These features are associated with obtaining a table of observations (4). Because in this case we consider a spatial model (at least at the level of initial data), one must highlight the spatial objects to be examined. Papers [11, 22] chose, as spatial objects, segments of an image. In many cases, the segments on digital images that are convenient to select are the rectangles, which are matched by a certain spatial region on the ground or on water area. The rectangular shape of an object is not mandatory; it could be different in other cases. We assume that each segment represents one state of the system at some time point. The components of system A_1, A_2,..., A_N, in a given case, are the colorimetric parameters. If we use a photograph in the RGB model, these parameters are calculated based on components R, G, B. It is also assumed that each segment considered in dynamics behaves as a dynamical system under the DMDS scheme, but different segments are at different steps along trajectory (1). Therefore, a given situation obeys the described identification scheme for DMDS model. Table of observations (4) is then a set of N colorimetric parameters while the number of columns in Table (4) corresponds to the number of segments. Identifying parameters for the dynamical system in line with (4), we obtain a notation of the dynamical process that generated these data.

This scheme has a series of unresolved issues. These include the selection of a segment size, determining their borders, highlighting (filtering) those segments data on which are in poor agreement with the assumed dynamics, which in turn may be due to data transmission errors, failures in photographic equipment, etc. Paper [22] resolved these issues heuristically, by employing a knowledge about the examined objects.

All of the above applies to the traditional identification of the model based on initial data. In the present study, another task is being solved – based on spatial data (a digital photograph), to identify spatial objects through their assignment to the corresponding step along the computed trajectory of a dynamical system that takes form (2). That would make it possible to assign a temporal sequence, which corresponds to the time sequence of trajectory (2), to spatial objects.

Hereafter we assume the starting system's components (that is, colorimetric parameters) to be quantitative, and we shall apply the Spearman matrix for identification.

In this case, the task on referring the observations from Table (4) to a step along the trajectory of system (2) is ambiguous in the following sense. For each component A_i the number of ranks used to calculate the Spearman correlation coefficient can amount to tens, hundreds, or a larger value (depending on the size and character of the sample). In this case, the number of levels K, employed when computing trajectory (2), is typically accepted small – from 3 to 5. Given this, the specified identification can be based on different approaches. We shall describe two of them.

1. Identification based on the maximum share of recognized observations.

Assume that one has a table of observations (4) and trajectory (2), identified based on it and the selected model. The number of levels K is fixed.

Denote

$$m_i = \min_{1 \le k \le B} C_{ik}, \quad M_i = \max_{1 \le k \le B} C_{ik}, \quad i = 1, 2, ..., N.$$

Thus, the observed value for each component A_i is in the interval $[m_i, M_i]$ (in essence, this is the spread of sampling $C_{ik}, \; k = 1, 2, ..., B$). Suppose that in (2) each component A_i accepts κ_i values. Employing the number κ_i is due to the following. Each component along the trajectory, according to the model, can accept K values, but for a specific trajectory the number of these values may be less than K. This actual number of values was denoted through κ_i.

Let $\mathbf{k}_i = \{v_i, v_i + 1, ..., v_i + \kappa_i - 1\}$ (all v_i are integers and positive, $i = 1, 2, ..., N$) be the values accepted by component A_i along the trajectory. We introduce function

$$\Psi: \; \mathbb{R}^N \mapsto \mathbf{k}_1 \times \mathbf{k}_2 \times ... \times \mathbf{k}_N,$$

that depends on $\kappa_1 + \kappa_2 + ... + \kappa_N - N$ parameters $\mu_{1,1}, \mu_{1,2}, ..., \mu_{1,\kappa_1-1}, \mu_{2,1}, \mu_{2,2}, ..., \mu_{2,\kappa_2-1}, ..., \mu_{N,1}, \mu_{N,2}, ..., \mu_{N,\kappa_N-1}$ (to reduce the notation, we omit the parameters when recording Ψ) and which is calculated in the following way:

$$\Psi(x_1, x_2, ..., x_N) = (k_1, k_2, ..., k_N), (k_1, k_2, ..., k_N) \in \mathbf{k}_1 \times \mathbf{k}_2 \times ... \times \mathbf{k}_N,$$

if and only if

$$
\begin{aligned}
& \mu_{1,k_1-1} \le x_1 < \mu_{1,k_1}, \\
& \mu_{2,k_2-1} \le x_2 < \mu_{2,k_2}, \\
& ... \\
& \mu_{N,k_N-1} \le x_N < \mu_{N,k_N},
\end{aligned}
\tag{5}
$$

at $x_i < \mu_{i,1}$ and $x_i \ge \mu_{i,k_i-1}$ conditions (5) are trivially supplemented by additional inequalities; we do not elaborate on the subject.

The essence of function $\Psi(\cdot, \cdot, ..., \cdot)$ is the computation of discrete vector $(k_1, k_2, ..., k_N) \in \mathbf{k}_1 \times \mathbf{k}_2 \times ... \times \mathbf{k}_N$ based on numerical vector $(x_1, x_2, ..., x_N)$. It follows from (5) that $\Psi(\cdot, \cdot, ..., \cdot)$ is a definite function. When computing it, parameters μ_{ij} are employed as thresholds, hence a condition

$$m_i < \mu_{i,1} < \mu_{i,2} < ... < \mu_{i,\kappa_i-1} < M_i, \; i = 1, 2, ..., N.$$

Consider trajectory (2). Its each column can be recorded as an element from set $\mathbf{k}_1 \times \mathbf{k}_2 \times ... \times \mathbf{k}_N$. We denote via $\mathbb{S}$ the totality of all such elements that correspond to columns (2). We shall derive an indicator function of totality $\mathbb{S}$ on set $\mathbf{k}_1 \times \mathbf{k}_2 \times ... \times \mathbf{k}_N$

$$\sigma_{\mathbb{S}}(\mathbf{k}) = \begin{cases} 1, \; if \; \mathbf{k} \in \mathbb{S}, \\ 0, \; if \; \mathbf{k} \notin \mathbb{S}. \end{cases}$$

Set the problem

$$\frac{1}{B} \sum_{k=1}^{B} \sigma_{\mathbb{S}}(\Psi(C_{1k}, C_{2k}, ..., C_{Nk})) \mapsto \max, \tag{6}$$

where max is taken based on parameters $\mu_{1,1}, \mu_{1,2}, ..., \mu_{1,k_1-1}, \mu_{2,1}, \mu_{2,2}, ..., \mu_{2,k_2-1}, ..., \mu_{N,1}, \mu_{N,2}, ..., \mu_{N,k_N-1}$, on which $\Psi(\cdot, \cdot, ..., \cdot)$ depends. The multiplier $1/B$ takes the normalizing role, eliminating the dependence of the maximized magnitude in (6) on the sample size, which may prove important when comparing models, based on different data. Essentially, problem (6) comes down to finding the thresholds μ_{ij}, which, through function $\Psi(\cdot, \cdot, ..., \cdot)$, make it possible to refer the maximum number of columns in matrix (4) to the states of the system included in trajectory (2). It follows from the properties of the maximized magnitude in (6) that a maximum is always achieved, however, the issue on the uniqueness of thresholds and, therefore, the uniqueness of values for $\Psi(C_{1k}, C_{2k}, ..., C_{Nk})$, requires additional study.

After we obtain parameters μ_{ij}, each observation $(C_{1k}, C_{2k}, ..., C_{Nk})$ in (4), which satisfies $\sigma_{\mathbb{S}}(\Psi(C_{1k}, C_{2k}, ..., C_{Nk})) = 1$, is assigned the state in (2) in line with rule

$$(C_{1k}, C_{2k}, ..., C_{Nk}) \mapsto \Psi(C_{1k}, C_{2k}, ..., C_{Nk}). \tag{7}$$

2. Identification based on the maximum proximity of correlations.

It is possible to find the threshold values for function $\Psi(\cdot, \cdot, ..., \cdot)$ based on a different principle. Assume that at certain fixed μ_{ij} we converted table (4) in line with rule:

$$\Psi(C_{1k}, C_{2k}, ..., C_{Nk}) = (\text{}_{1k}, \text{}_{2k}, ..., \text{}_{Nk}), \quad k = 1, 2, ..., B.$$

Following such a transform, $\tilde{M}$ is recorded in the form

$$\hat{M} = \begin{pmatrix} c_{11} & c_{12} & ... & c_{1B} \\ c_{21} & c_{22} & ... & c_{2B} \\ ... & ... & ... & ... \\ c_{N1} & c_{N2} & ... & c_{NB} \end{pmatrix},$$

considering that function $\Psi(\cdot, \cdot, ..., \cdot)$ maps a vector-column into a vector-column.

Each line i in matrix $\hat{M}$, similar to trajectory (2), has no more than κ_i different values. We find $\hat{P}$ – a correlation Spearman matrix between lines $\hat{M}$.

Set the problem – it is required to find a minimum for all possible sets of parameters μ_{ij}

$$\sum_{i=1}^{N-1} \sum_{j=i+1}^{N} \left([P]_{ij} - [\hat{P}]_{ij} \right)^2 \mapsto \min.$$

Thus, based on the initial table (4), we find a matrix of discrete values $\hat{M}$, which has the closest correlation matrix, in the sense of magnitude $\sum_{i=1}^{N-1} \sum_{j=i+1}^{N} \left([P]_{ij} - [\hat{P}]_{ij} \right)^2$ (correlations are computed among lines), to the correlation matrix P.

For the reasons given above, one can say that a given minimum is reached, however the issue on the uniqueness of parameters requires further study.

The found function $\Psi(\cdot, \cdot, ..., \cdot)$ allows us to proceed from Table (6) to the trajectory matrix in line with the previous rule (7).

A special case worthwhile mentioning is when function $\Psi(\cdot, \cdot, ..., \cdot)$ assigns, for some of the columns in observation matrix (4), a vector that is not included in totality $\mathbb{S}$, that is, when it is impossible to assign the state along trajectory (2) to an observation. Such a situation is possible; it can be predetermined by a series of circumstances. It is possible that discretization of the model defined by number K does not make it possible to carry out the specified classification. In the examined case, when using a color RGB-model, values for components belong to the quantitative scale (in most software packages, 32- and 64-bit real values, sometimes

8-bit integers). However, the number of levels along the trajectory is small, typically not more than 5. Another possibility is when an observation in (4) accepts a certain intermediate value between the states of the trajectory. Finally, there may be errors in the source data that pose the same problem.

In practice, an observation that is not identified with the state of a dynamical system can be either neglected or, by using the approaches accepted in clustering, be attributed to a certain close state.

Thus, the procedure for constructing a spatial model based on a digital photograph can be expressed by the following scheme:

1) split the original image into segments (spatial objects);

2) compute colorimetric parameters for all segments and compile a table of observations (4);

3) identify parameters of the dynamic model, the result being the computed trajectory (2);

4) use a procedure for attributing an observation to the state of the system when each observation in (4) is assigned with the state or the number of the step along trajectory (2);

5) visualize obtained results, making it possible to derive a spatial pattern of the restored dynamics.

5. Application of the spatial-dynamic model to a digital photograph of the cluster of toxic cyanobacteria

A source material for the computational implementation of the model was a digital photograph of CTC [12], shown in Fig. 1.

Fig. 1. A flowering spot is the accumulation of toxic cyanobacteria in the Baltic Sea

The image was split into 15 (horizontal)×10 (vertical)=150 segments (spatial objects). In this case, construction of the spatial-dynamic model employed 100 segments, which unambiguously belonged to the spot. 50 segments showing the open water (top right corner and bottom left) were excluded from the analysis. The excluded segments are displayed in the photograph with modelling results.

For each of 100 segments we computed average (per a segment) values for the intensity of RGB components, which are denoted: R, G, B. By using these averages, we computed colorimetric parameters of specific hydrobiological meaning, essential for a given object:

$R/(R+G+B)$ – this parameter is related to the number of orange-yellow and red pigments that are prevalent in the old and dead cells in most photosynthesizing organisms, including cyanobacteria;

$G/(R+G+B)$ – this parameter is related to the amount of the green pigment chlorophyll, which determines the level of photosynthetic productivity;

$G/(R+G)$ – this parameter is an indicator of ratio of the magnitude of photosynthetic products to the total, dead and alive, biomass of plant communities;

R/G – this parameter demonstrates the pigment diversity of phytoplankton associated with its stability.

We have chosen for the identification a discrete model based on the Liebig's law, with the number of discrete levels of components taken as $K=3$.

For the purposes of this study, it would suffice to calculate trajectory (2), which is why the structure of component-to-component-relations, also the result of simulation, is neglected. The trajectory of the system is given in Table 1. The rows correspond to the specified colorimetric parameters that have three levels in a given model ($K=3$). These levels can be interpreted as low (1), middle (2), and high (3).

Table 1

Trajectory of the system, representing a cycle in the change of values for colorimetric parameters of a cluster of toxic cyanobacteria, shown in Fig. 1. t is the discrete time

R/(R+G+B)	3	3	3	2	1	1	1	2
G/(R+G+B)	1	2	3	3	3	2	1	1
G/(R+G)	1	1	1	2	2	2	2	1
R/G	2	2	2	1	1	1	1	2
t	1	2	3	4	5	6	7	8

In order to construct a spatial-temporal model, we employed the identification based on the maximal share of identified observations. It follows from Table 1 that the number of levels κ_i for components $R/(R+G+B)$, $G/(R+G+B)$, $G/(R+G)$, R/G are equal, respectively, to 3, 3, 2, 2. Thus, the number of parameters μ_{ij} is equal to 6 (=3+3+2+2−4).

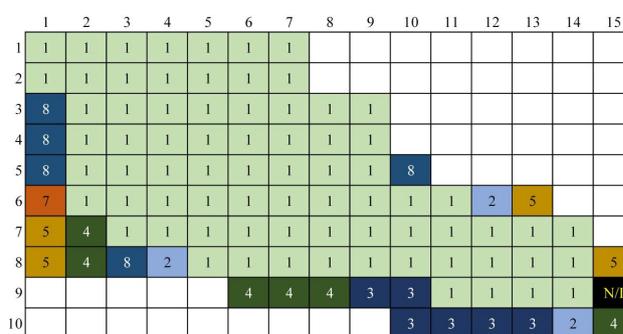Fig. 2 shows a spatial-temporal pattern, corresponding to the model.

Fig. 2. A spatial-dynamical structure of a flowering spot shown in Fig. 1. Spatial objects (rectangles) contain numbers that correspond to their chronological order according to the trajectory of the system in Table 1. The rectangles with the same numbers are colored similarly. N/I is the unidentified segment. The objects excluded from the analysis are shown by white rectangles without a number

We should pay attention to the following. When constructing a spatial-temporal pattern, we registered no observation that corresponds to time $t=6$. Out of 100 spatial objects, only one was not identified. Values for components $R/(R+G+B)$, $G/(R+G+B)$, $G/(R+G)$, R/G for it are equal, respectively, to 0.235, 0.390, 0.624, 0.603. By using the

above procedure based on clustering, one can find a close state of the system for it as well.

The constructed model allows us to apply the following hydrobiological treatment. In the trajectory of the system (Table 1), one can isolate a series, hereafter called the "productive", consisting of steps at t=2, 3, 4, 5. In this series, we observe an increase in the values for colorimetric parameter $G/(R+G)$ at a simultaneous decrease in the values for colorimetric parameter R/G. Such dynamics in the specified colorimetric parameters are matched with a certain series of alternating strategies in the functioning of CTC plant community. This series is characterized by an increase in the photosynthetic productivity of CTC biosystem and by a decrease in its stability (a sign of which is the reduction of pigment diversity). In this series, there is also a reduction in the red component of CTC color (colorimetric parameter $R/(R+G+B)$) at a simultaneous increase in the green component (colorimetric parameter $G/(R+G+B)$). This is a manifestation of processes that give rise to the living, actively photosynthesizing biomass, while decomposing the dead. Decomposition of the dead biomass saturates water with nutrients, required for the growth of living biomass.

The series, hereafter called the "stabilizing", includes steps with numbers t=6, 7, 8, 1 (because the dynamics are periodic, point 8 is followed by point 1). In this series, there is a decrease in the values for colorimetric parameter $G/(R+G)$ at a simultaneous increase in the values for colorimetric parameter R/G. Such dynamics of the specified colorimetric parameters are matched with another series of alternating strategies. This series is characterized by a decrease in the photosynthetic productivity of CTC biosystems and an increase in its stability (a sign of which is the increased pigment diversity). In this series, there is also an increase in the red component of CTC color (colorimetric parameter $R/(R+G+B)$) at a simultaneous decrease in the green component (colorimetric parameter $G/(R+G+B)$). This is a manifestation of the die-out processes of living biomass and the accumulation and preservation of biogenic elements in the dead.

The specified series of strategies in the spatial structure of CTC correspond to the zones of: production and stabilization.

Fig. 2 shows that the stabilization zone occupies the central area of CTC, from the upper-left corner of the image to the right bottom. Water exchange occurs under relatively unfavorable conditions within it.

Production zones are the periphery of CTC, where conditions for water exchange and for supplying nutrients to the living biomass are better.

Thus, the simulation results correspond to known biological and physical-chemical regularities in the functioning of aquatic plant communities [24].

The following illustrations show the structure of CTC in coastal waters. In order to identify them, we also selected a model with the approach based on the Liebig's law and the number of levels of components K=3. The structure of these clusters has a series of features associated with the shallow depth of the water reservoir and the proximity to the bank.

The image was split into 300 segments; we then repeated the procedure described for the image in Fig. 1. The trajectory of colorimetric parameters is given in Table 2; the spatial structure is shown in Fig. 4.

Fig. 3. Cluster of cyanobacteria at the river Sudbury, Massachusetts, United states [25]

Table 2

A cycle of change in the colorimetric parameters of the cluster of toxic cyanobacteria, shown in Fig. 3

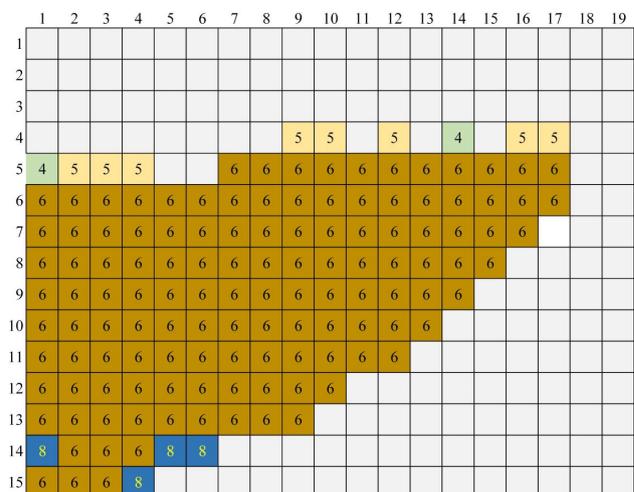| R/(R+G+B)	1	1	1	1	1	1	2	2
G/(R+G+B)	2	1	1	1	2	3	3	3
G/(R+G)	1	1	2	3	3	3	2	1
R/G	3	3	2	1	1	1	2	3
t	1	2	3	4	5	6	7	8

Fig. 4. Spatial objects, identified according to the trajectory of the system from Table 2. Notation is similar to Fig. 2

Some steps of the cycle (Table 2) did not find any matching among image segments in Fig. 4. The reasons for this were partly discussed above. A similar property is also characteristic of the structure of other CTCs analyzed below.

The structure in Fig. 4 can be given the following hydrobiological treatment. Step 8 corresponds to the high system's stability (for parameter R/G), although it is low, relative to the total biomass, in terms of photosynthetic productivity (for parameter $G/(R+G)$), a relatively high ratio of dead cells to the living cells (ratio of $R/(R+G+B)$ to $G/(R+G+B)$). This state is matched by a relatively weak vulnerability of CTC to the treatment by means that preclude the photosynthetic

productivity, hence the high sensitivity of cyanobacteria to external influences, for example, treatment with algaecides that eliminate photosynthesis.

Fig. 4 shows a qualitative effect due to the location of segments in such a state closer to the bank than segments for steps 4, 5, 6. The latter steps are characterized by relatively low values of stability and high values of productivity for the same indicators at low values of the number of dead cells and an increase in the value for the number of living cells.

Fig. 5. Cluster of cyanobacteria at the coastal strip of a water reservoir [26]

Split into 300 segments; the trajectory of colorimetric parameters is in Table 3; the spatial structure is in Fig. 6.

Table 3

A cycle of change in the colorimetric parameters for the cluster of toxic cyanobacteria, shown in Fig. 5

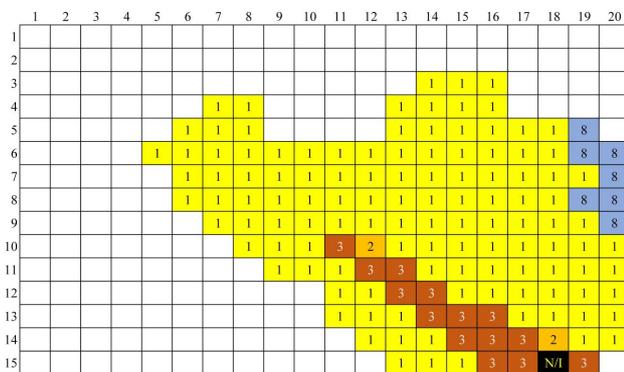| R/(R+G+B)	3	3	3	2	1	1	1	1	2
G/(R+G+B)	1	2	3	3	3	2	1	1	1
G/(R+G)	1	1	1	2	2	2	2	1	1
R/G	2	2	2	1	1	1	1	2	2
t	1	2	3	4	5	6	7	8	9

Fig. 6. Spatial objects, identified according to the trajectory of the system from Table 3. Notation is similar to Fig. 2

In Fig. 5, the state (step 1) that is characterized by the maximum prevalence of dead cells over the living cells corresponds to the coastal areas. Step 8 corresponds to the areas bordering on the open water, where such a prevalence is not observed.

Split into 216 segments, the trajectory of colorimetric parameters is in Table 4; the spatial structure is shown in Fig. 8.

Fig. 7. Cluster of cyanobacteria at the coastal strip of a water reservoir [27]

Table 4

A cycle in the change of colorimetric parameters for the cluster of toxic cyanobacteria, shown in Fig. 7

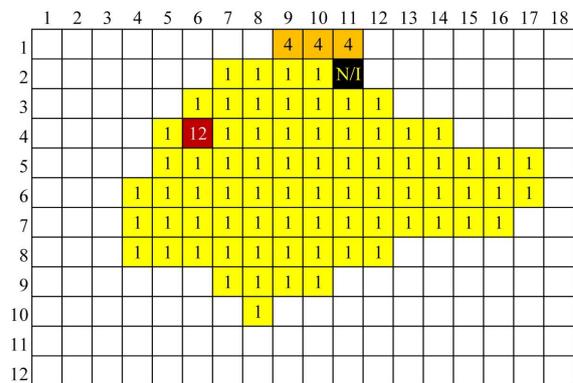| R/(R+G+B)	2	3	3	3	3	3	2	1	1	1	1	1
G/(R+G+B)	3	3	3	3	2	1	1	1	1	1	2	3
G/(R+G)	3	3	2	1	1	1	1	1	2	3	3	3
R/G	1	1	2	3	3	3	3	3	2	1	1	1
t	1	2	3	4	5	6	7	8	9	10	11	12

Fig. 8. Spatial objects, identified according to the trajectory of the system from Table 4. Notation is similar to Fig. 2

In Fig. 8 we observe a pattern similar to that shown in Fig. 6. Step 4 with low productivity and high stability, as well as the proportion of dead cells that is relatively higher in comparison with other steps, corresponds to coastal areas. The areas that are more distant from the bank (steps 1 and 12) are matched by states with high productivity and low stability at a relatively lower proportion of the dead organic matter.

In Fig. 9, the location of a coastal area can be identified by the reflection of trees in the upper left corner of the image. Split into 180 segments; the trajectory of colorimetric parameters is in Table 5; the spatial structure is shown in Fig. 10.

In Fig. 10, we also observe the states at the coastal areas (steps 6, 8) with low productivity and high stability. At areas remote from the bank (steps 1, 2), we observe high productivity and low stability.

Fig. 9. Cluster of cyanobacteria at Lake Mendota, Wisconsin, United States [28]

Table 5

A cycle in the change of colorimetric parameters for the cluster of toxic cyanobacteria, shown in Fig. 9

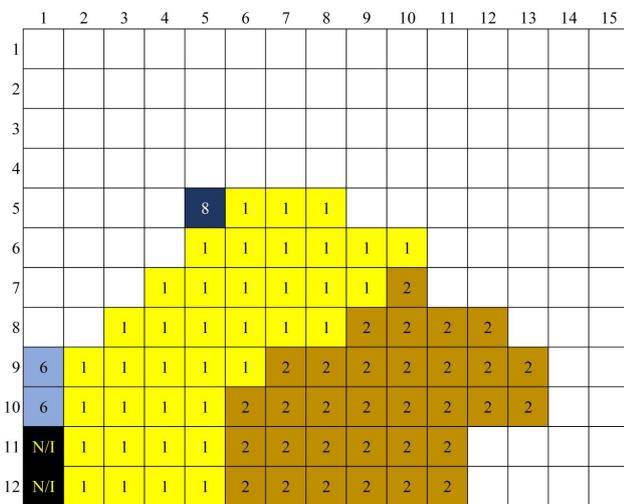| R/(R+G+B)	3	3	3	2	1	1	1	1	2
G/(R+G+B)	1	2	3	3	3	2	1	1	1
G/(R+G)	1	1	1	2	2	2	2	1	1
R/G	2	2	2	1	1	1	1	2	2
t	1	2	3	4	5	6	7	8	9

Fig. 10. Spatial objects, identified according to the trajectory of the system from Table 5. Notation is similar to Fig. 3

6. Discussion of results of the spatial-dynamical modelling of clusters of toxic cyanobacteria

The spatial-dynamical model, constructed in this study, is based on the following patterns. The examined spatial objects are treated as separate implementations of a certain dynamic system with the deterministic dynamics corresponding to conditions in a given space domain. These objects differ only by their own time, which is identified using the described methods. Thus, the dynamics of objects can be restored based on spatial data, and the main result of this study is the construction of a mathematical model that makes it possible to restore the temporal arrangement for spatial objects.

The key results of our work are as follows.

1. The highlighted colorimetric parameters for a digital photograph of CTC will make it possible to establish the character of bioproduction processes in different clusters. These parameters are derived based on the RGB color model; they describe such characteristics of bioproduction processes as the number of pigments, the level of photosynthetic productivity, the ratio of magnitude of photosynthetic production to the biomass of plant communities, an indicator of the pigment diversity of phytoplankton.

2. The devised procedure for the identification of spatial objects in a two-dimensional image of CTC based on a digital photograph enables finding the correspondence between segments of the image and steps in the trajectory of the dynamic model DMDS. Thus, the specified identification restores the spatial-dynamical pattern of bioproduction processes related to accumulation. We have developed two variants of the spatial-dynamical model based on the maximal share of identified observations and the maximal proximity of correlations.

3. We have verified the model using a series of photographs of the clusters of cyanobacteria in the Baltic Sea and at coastal sites of water reservoirs. The approbation has shown that when the model is applied, almost all segments in the image are identified with the respective phases in the bioproduction process. In our opinion, this testifies to the sufficient adequacy of the model to the studied phenomenon. The resulting structure of the cyanobacteria cluster allows us to draw practical conclusions in order to organize activities for eliminating the biological threat posed by CTC (for instance, treatment with chemicals).

The constructed model opens up new perspectives in the development of remote sensing of CTC owing to the combination of two of its main features. First, a local analysis (at a segment, a plot) of the character of bioproduction processes employs the colorimetric parameters acquired from a digital photograph. Second, the restoration of the spatial arrangement uses a dynamic pattern, which adequately describes the progress of these processes in the cyanobacteria cluster.

The merits of the proposed solution include a possibility to identify the spatial location of cluster sites, in line with various chronological phases in the bioproduction processes. As noted in our review of the scientific literature, at present the analysis of CTC employs sophisticated spectral methods, which, in principle, make it possible to explore the bioproduction processes through analysis of the colorimetric parameters of images. However, these methods are static, they do not take into consideration the complex dynamics of cyanobacteria clusters and, for the time being, enable the reliable determination of clusters' boundaries only, without accounting for their internal structure.

It makes sense to note several constraints for the proposed model, as well as ways to overcome them and to improve the model. As pointed in publications on a DMDS model [21, 22], identification of the model with high dimensionality (many components and levels) is a computationally challenging task. It is possible to partially overcome this obstacle by using specialized optimization techniques, such as evolutionary algorithms, however, for a given class of problems, it is still not clear how an extremum, derived from these methods, differs from the actual one. In general, solving the problems of high dimensionality requires the development of effective algorithms that would find solutions at acceptable cost.

To be specially considered are also the methods for identification of sites where cyanobacteria accumulate. In this work, mainly for reasons of convenience, we considered

the simplest type of segments with a rectangular shape. The further development of the method would probably require consideration of segments of arbitrary shape, which could be identified at steps of the trajectory of a dynamical system. This may require designing the new methods of image segmentation, which would be appropriate for a given model.

The significance of the results obtained should be assessed relative to the issue on eliminating the threats to biosecurity under certain extreme situations associated with the emergence of clusters of toxic cyanobacteria at large water areas. In some cases, the information is required not only about their coordinates and parameters of motion, but also about the structure, which is especially important in case of the emergence of CTC with particularly toxic mutants of cyanobacteria. In such situations, it may be justified to apply radical measures to fight CTC, such as treating them with algaecides from air. There will be a need to determine the areas of accumulation at which the specified measures could prove most effective. The results of our work form preconditions for the development of a technology for operative determination of such sites. The advantage of this technology is the possibility of remote control when using aerospace methods for detecting these sites.

Currently, there are big volumes of data on different aspects of bioproduction processes in the phytoplankton of marine waters and biological communities, which it is a part of it. These rather detailed data were acquired by non-remote methods. The results of this work provide an opportunity to design the remote technology for determining the character of bioproduction processes. Comparing it with the non-remote methods reveals the following pattern.

Non-remote methods enable obtaining more detailed data about bioproduction processes. Remote sensing makes it possible to operatively acquire data on vast water areas over tens or hundreds of miles. However, they provide only the most general idea about ratios of processes of photosynthetic production, accumulation and the die-out of dead organic matter. These data, however, would suffice, for example, to detect the clusters where algaecide treatment at a given time is not advisable. We note that modern satellite-based methods for detection of CTC, described in papers from our review, do not make it possible to contribute to the same general understanding and provide information only about the size of clusters, enabling the estimation of the total amount of the living and dead biomass of cyanobacteria.

Application of the proposed spatial-dynamical model would implement the benefits of remote sensing methods in the above-mentioned emergencies, when it is necessary under time constraints to decide on tactics and strategy to deal with CTC.

7. Conclusions

1. We have defined the colorimetric parameters (related to the amount of pigments, chlorophyll, and other biochemical indicators) that make it possible to identify the character of bioproduction processes in a cluster. These parameters could be computed based on a digital photograph, acquired by aerospace methods. The essence of this result is that the bioproduction processes are examined remotely, without referring to methods of laboratory biochemical diagnosis.

2. We have constructed an algorithm for the identification of an image segment showing the state of a dynamical system that corresponds to a cluster. This makes it possible to specify to which step along the trajectory of a dynamical system a particular area of accumulation corresponds to. That yields important information about the dynamics of changes in a cluster, making it possible to separate those areas in which it is most appropriate to implement measures in order to eliminate biothreats. The essence of the algorithm for identifying the segments is to split the scale of changes in the colorimetric parameters into numeric intervals corresponding to the levels of these parameters along the trajectory of a dynamical system. Such a split can be performed in any number of techniques. In this work, the two approaches to splitting have been proposed. Under a first approach, the borders of intervals that divide the scale of a colorimetric parameter ensure the maximal share of the identified segments in their total number. Under a second approach, the borders minimize the measure that reflects the proximity of actual data with values for components calculated according to the algorithm of identification.

3. The devised spatial-dynamical model has been verified using 5 digital images of CTC in order to determine the structure of clusters. A variant of the model, based on the maximal share of identified segments, made it possible to identify almost all segments in the image. The share of unidentified segments for different photographs ranges from 0 to 2.8 %. This indicator could be considered as evidence of the adequacy of the model. A detailed analysis of the structure of a cluster, identified based on a photograph of CTC in the Baltic Sea, detected two phases, reflected in the trajectory. The greatest threat, in terms of biosecurity, is posed by the phase that we denoted "productive". This phase was matched by 19 segments out of 100. The phase consists of segments in four states, which points t=2, 3, 4, 5 in the trajectory correspond to (Table 1) with the number of segments 3, 6, 6, and 4, respectively. It is obvious that the choice of sites for the implementation of measures on the elimination of toxicity requires separate consideration, taking into account a variety of factors. However, the above indicator testifies to the model's capability to separate at the surface of a cluster a small area where application of biosafety measures would be most appropriate.

4. The model allows the extension to a spatial structure of arbitrary dimensionality, since the concept of the model implies the representation of a spatial object in the form of a corresponding dynamic system. The extension is also possible in the direction of development of methods for linking spatial objects to the phases in a dynamic process. Because the dynamical pattern of the model is represented by DMDS model, which is itself a complex multiparameter dynamic system, an important step in improving the proposed spatial-temporal model should be the parametric adjustment that would account for all biochemical, hydrobiological, physical information about a cluster, rather than a digital photograph only.

References

1. Bukvareva E., Aleshchenko G. Optimization, Niche and Neutral Mechanisms in the Formation of Biodiversity // American Journal of Life Sciences. 2013. Vol. 1, Issue 4. P. 174–183. doi: https://doi.org/10.11648/j.ajls.20130104.16

2. Margalef R. Perspectives in Ecology Theory. University of Chicago Press, 1968. 112 p.

3. Annual Reports 1969–2013 / T. Berman, C. Serruya, M. Gophen, A. Sukenik, T. Zohary (Eds.). LKDB-KLL, 2013.

4. Karabashev G. S., Evdoshenko M. A. Spektral'nye priznaki cveteniya cianobakteriy v Baltiyskom more po dannym skanera MODIS // Sovremennye Problemy Distancionnogo Zondirovaniya Zemli iz Kosmosa. 2015. Vol. 12, Issue 3. P. 158–170.

5. Bioterrorism: New Technologies for Global Emergencies and Public Health / Mugavero R., Sabato V., Basso M., D'Amico W., Benolli F. // Journal of Information Privacy and Security. 2015. Vol. 11, Issue 4. P. 262–273. doi: https://doi.org/10.1080/15536548.2015.1105658

6. Tekhnologiya monitoringa sostoyaniya posevov po dannym distancionnogo zondirovaniya Zemli na yuge Zapadnoy Sibiri / Sladkih L. A., Zahvatov M. G., Saprykin E. I., Saharova E. Yu. // Geomatika. 2016. Issue 2. P. 39–48.

7. Terekhin E. A. NDVI seasonal dynamics of perennial grasses and its use for classification of their crops in the Belgorod region // Sovremennye Problemy Distancionnogo Zondirovaniya Zemli iz Kosmosa. 2015. Vol. 12, Issue 1. P. 9–17.

8. Mitchell A. L., Rosenqvist A., Mora B. Current remote sensing approaches to monitoring forest degradation in support of countries measurement, reporting and verification (MRV) systems for REDD+ // Carbon Balance and Management. 2017. Vol. 12, Issue 1. doi: https://doi.org/10.1186/s13021-017-0078-9

9. Carbon-based phytoplankton size classes retrieved via ocean color estimates of the particle size distribution / Kostadinov T. S., Milutinović S., Marinov I., Cabré A. // Ocean Science. 2016. Vol. 12, Issue 2. P. 561–575. doi: https://doi.org/10.5194/os-12-561-2016

10. Development of the descriptive binary model and its application for identification of clumps of toxic cyanobacteria / Nosov K., Zholtkevych G., Georgiyants M., Vysotska O., Balym Y., Porvan A. // Eastern-European Journal of Enterprise Technologies. 2017. Vol. 4, Issue 4 (88). P. 4–11. doi: https://doi.org/10.15587/1729-4061.2017.108285

11. Bespalov Y., Nosov K., Kabalyants P. S. Modeling systemic colorimetric parameters as a tool for processing images of clumps of toxic cyanobacteria targeted at their boundaries detection // bioRxiv. 2017. doi: https://doi.org/10.1101/232413

12. Lavrova O. Yu., Mityagina M. I., Kostianoy A. G. Kostianoy Satellite Methods for Detecting and Monitoring Marine Zones of Ecological Risk. Moscow: IKI RAN, 2016. P. 45–47.

13. Darmofal D. Spatial Analysis for the Social Sciences. Cambridge University Press, 2015. doi: https://doi.org/10.1017/cbo9781139051293

14. Banerjee A., Ray S. Spatial Models and Geographic Information Systems // Encyclopedia of Ecology. 2019. P. 178–188. doi: https://doi.org/10.1016/b978-0-12-409548-9.11237-0

15. Wang T., Wang R. A network-city model of spatial competition // Economics Letters. 2018. Vol. 170. P. 168–170. doi: https://doi.org/10.1016/j.econlet.2018.06.023

16. Spatial model of a pyrophite shrub in Mediterranean terrestrial ecosystems / Usó-Doménech J.-L., Nescolarde-Selva J.-A., Lloret-Climent M., González-Franco L., Alonso-Stenberg K. // Ecological Modelling. 2018. Vol. 384. P. 333–340. doi: https://doi.org/10.1016/j.ecolmodel.2018.06.030

17. Spatial modelling of the regulating function of the Huangqihai Lake wetland ecosystem / Fu Y., Zhao J., Peng W., Zhu G., Quan Z., Li C. // Journal of Hydrology. 2018. Vol. 564. P. 283–293. doi: https://doi.org/10.1016/j.jhydrol.2018.07.017

18. D'Silva J. P., Eisenberg M. C. Modeling spatial invasion of Ebola in West Africa // Journal of Theoretical Biology. 2017. Vol. 428. P. 65–75. doi: https://doi.org/10.1016/j.jtbi.2017.05.034

19. Dynamic spatio-temporal models for spatial data / Hefley T. J., Hooten M. B., Hanks E. M., Russell R. E., Walsh D. P. // Spatial Statistics. 2017. Vol. 20. P. 206–220. doi: https://doi.org/10.1016/j.spasta.2017.02.005

20. Wheeler D. C., Waller L. A. Mountains, valleys, and rivers: The transmission of raccoon rabies over a heterogeneous landscape // Journal of Agricultural, Biological, and Environmental Statistics. 2008. Vol. 13, Issue 4. P. 388–406. doi: https://doi.org/10.1198/108571108x383483

21. Discrete Modeling of Dynamics of Zooplankton Community at the Different Stages of an Antropogeneous Eutrophication / Zholtkevych G. N., Bespalov G. Y., Nosov K. V., Abhishek M. // Acta Biotheoretica. 2013. Vol. 61, Issue 4. P. 449–465. doi: https://doi.org/10.1007/s10441-013-9184-6

22. Descriptive Models of System Dynamics / Zholtkevych G. N., Nosov K. V., Bespalov Y. G., Rak L. I., Vysotskaya E. V., Balkova Y. B., Kolomiychenko V. K. // Communications in Computer and Information Science. 2017. P. 97–114. doi: https://doi.org/10.1007/978-3-319-69965-3_6

23. Mathematical modeling of systemic colorometric parameters unmasking wild waterfowl / Balym Y., Vysotska O., Pecherska A., Bespalov Y. // Eastern-European Journal of Enterprise Technologies. 2017. Vol. 5, Issue 2 (86). P. 12–18. doi: https://doi.org/10.15587/1729-4061.2017.110107

24. Handbook of Marine Microalgae / S.-K. Kim (Ed.). Academic Press, 2015. 604 p. doi: https://doi.org/10.1016/c2013-0-19117-9

25. Monitoring and Responding to Cyanobacteria and Cyanotoxins in Recreational Waters. URL: https://www.epa.gov/nutrient-policy-data/monitoring-and-responding-cyanobacteria-and-cyanotoxins-recreational-waters

26. Toxic Cyanobacterial Blooms. URL: https://www.nalms.org/nalms-position-papers/toxic-cyanobacterial-blooms

27. Cyanobacteria blooms found in Forge Pond and Peconic Lake; health officials warn residents to stay out of the water. URL: https://riverheadlocal.com/2016/07/11/cyanobacteria-blooms-found-forge-pond-peconic-lake-health-officials-warn-residents-stay-water

28. Toxic Algae, Drinking Water and Why Madison Won't be Toledo. URL: https://yaharawsc.wordpress.com/2014/08/05/toxic-algae-drinking-water-and-why-madison-wont-be-toledo